Available online at www.sciencedirect.com
ScienceDirect
Carbohydrate Polymers 68 (2007) 740–745
Carbohydrate Polymers
www.elsevier.com/locate/carbpol

Preparation and physicochemical properties of a novel hydroxyapatite/chitosan–silk fibroin composite

Li Wang, Chunzhong Li *

Key Laboratory for Ultrafine Materials of Ministry of Education, School of Materials Science and Engineering, East China University of Science and Technology, P.O. Box 258, 130 Meilong Road, Shanghai 200237, PR China

Received 5 April 2006; received in revised form 31 July 2006; accepted 15 August 2006
Available online 29 September 2006

Abstract

A novel hydroxyapatite/chitosan–silk fibroin (HA/CTS–SF) composite was prepared for bone repair and replacement by a coprecipitation method. It was revealed that the inorganic phase in the composite was carbonate-substituted HA with low crystallinity. The HA crystallites were found to be needle-like in shape with a typical size of 20–50 nm in length and around 10 nm in width. The composite exhibited a higher compressive strength than the precipitated HA without any organic source involved, which was closely related to the perfect incorporation of chitosan and SF macromolecules into the composite. The chemical interactions occurring between the mineral phase and the organic matrix were thought to improve the interfacial bonding and thus resulted in the enhanced mechanical property of the composite.

Keywords: Hydroxyapatite; Chitosan; Silk fibroin; Composite; Chemical interaction; Compressive strength

1. Introduction

Natural bone is a complex inorganic–organic nanocomposite material, in which hydroxyapatite (HA) nanocrystals and collagen fibrils are well organized into hierarchical architecture over several length scales (Du et al., 2000; Kikuchi, Itoh, Ichinose, Shinomiya, & Tanaka, 2001). The distinctive harmony and the highly ordered assembly at the molecular level between the mineral phase and the organic matrix endow natural bone with good mechanical properties, such as low stiffness, high resistance to tensile and compressive forces, appreciable flexibility and high fracture toughness (Song, Saiz, & Bertozzi, 2003; Zhang, Liao, & Cui, 2003). However, exploiting bone grafting materials with microstructure and mechanical properties comparable to native bone poses a significant challenge in tissue engineering. Natural bone's unique hybrid composition and hierarchical structure, have presented valuable clues to achieve intelligent scaffold materials (Mann & Ozin, 1996; Stupp & Braun, 1997). Increasing efforts have been devoted to the composites of HA in conjugation with some bioactive polymers or proteins, such as collagen (Chang, Ikoma, Kikuchi, & Tanaka, 2002; Du et al., 2000; Kikuchi et al., 2001, 2004; Zhang et al., 2003), gelatin (Bigi, Panzavolta, & Roveri, 1998; Chang, Ko, & Douglas, 2003), chitosan (Murugan & Ramakrishna, 2004; Rusu et al., 2005; Sailaja et al., 2003; Yamaguchi et al., 2001; Zhang et al., 2005), silk fibroin (Furuzono, Taguchi, Kishida, Akashi, & Tamada, 2000; Wang, Nemoto, & Senna, 2002) and chondroitin sulfate (Rhee & Tanaka, 2002). Combining the advantages of inorganic and organic components (Sivakumar, Manjubala, & Rao, 2002), HA/organic composites show good biocompatibility and favorable bonding ability with surrounding host tissues inherent from HA (Hench, 1991; Nunes, Simske, Sachdeva, & Wolford, 1997). Besides, the problems associated with HA ceramic, such as its intrinsic brittleness, poor formability and migration of HA particles from the implanted sites (Murugan & Ramakrishna, 2004; Yamaguchi et al., 2001), can be circumvented by the

* Corresponding author. Tel.: +86 21 64252055; fax: +86 21 64250624.
E-mail address: czli@ecust.edu.cn (C. Li).

0144-8617/$ - see front matter © 2006 Elsevier Ltd. All rights reserved.
doi:10.1016/j.carbpol.2006.08.010

integration of HA ceramic with biopolymers. Among these HA-based hybrid materials, HA-collagen composite has inspired great interest because it bears a very close compositional resemblance to natural bone. Kikuchi et al. prepared a self-organized HA-collagen nanocomposite by a biomimetic coprecipitation method (Kikuchi et al., 2001, 2004). It was reported that the composite had similar microstructure to native bone, and showed osteoclastic resorption and good osteoconductivity as proved by the animal tests. However, a major concern over HA-collagen composite is the high cost of collagen, which limits its clinical application in healing bone defects.

Silk fibroin (SF), a hard protein extracted from silk cocoon, is composed of 17 amino acids. SF with β-sheet structure has been applied in wound dressing owing to its sufficient mechanical strength, appreciable bioaffinity, and good oxygen permeability similar to human skin (Freddi, Monti, Nagura, Gotoh, & Tsukada, 1997; Park, Lee, Ha, & Park, 1999). In our previous studies, HA–SF nanocomposite was obtained by a coprecipitation method (Wang et al., 2002, Wang, Nemoto, & Senna, 2004). It was shown that a three-dimensional porous network was constructed in the composite by the crosslinkage between HA clusters and SF fibrils and the introduction of SF notably increased the microhardness of HA ceramic. However, HA–SF composite cannot meet the requirement for bone substitution due to its insufficient formability and flexibility.

Chitosan, the deacetylation derivative of chitin, is a natural polysaccharide containing active amino and hydroxyl groups. Chitosan consists of glucosamine and *N*-acetylglucosamine units linked through 1–4 glycosidic bonds. Chitosan's primary attractive features including its biocompatibility, biodegradability, flexibility adhesiveness and anti-infectivity, make it as a feasible wound healing agent and an ideal polymeric matrix for HA ceramic (Murugan & Ramakrishna, 2004; Rusu et al., 2005; Sailaja et al., 2003; Yamaguchi et al., 2001). The brittleness of HA ceramic can be mitigated by the incorporation of chitosan into HA ceramic by virtue of the plastic and adhesive origin of chitosan. As an article by Yamaguchi et al. stated, the as-prepared chitosan/HA composite was mechanically flexible and could be easily molded into any desired shape (Yamaguchi et al., 2001). Bearing the above points in mind, we employed chitosan and SF together as a complex organic matrix for HA granules attempting to obtain a novel composite HA/chitosan–silk fibroin (HA/CTS–SF) with good osteoconductivity, enhanced mechanical strength and sufficient formability and flexibility. Additionally, chitosan and SF are easily derived from naturally abundant chitin and silk cocoon, respectively, which offers a great promise for the potential use of HA/CTS–SF composite as bone scaffold material.

In this work, HA/CTS–SF composite was synthesized by the coprecipitation method in the presence of chitosan and SF. The effects of the chitosan and SF on the crystallographic properties of HA were evaluated. The compressive strength of the composite and the chemical interaction between the mineral phase and the organic matrix were investigated.

2. Materials and methods

2.1. Preparation of HA/CTS–SF composites

$Ca(OH)_2$, H_3PO_4 and ammonium hydroxide of analytical grade were used without further purification. Chitosan with deacetylation degree of 80% and viscosity of 0.2 Pas was purchased from Sigma–Aldrich Inc., USA. SF superfine powders with β-sheet structure extracted from silk cocoon were kindly supplied by Wuxi Smiss Technol. Co., Ltd., China.

HA is formed at alkaline conditions (pH 9–11) according to the following equation

$$10Ca(OH)_2 + 6H_3PO_4 \rightarrow Ca_{10}(PO_4)_6(OH)_2 + 18H_2O \quad (1)$$

With the inorganic/organic weight ratio (70/30) of natural bone as a guideline, the weight ratio of HA/CTS/SF in the final product was regulated to be 70/15/15. According to the pre-determined theoretical yield of HA 14.00 g, the amount of every reagent initially used was calculated, i.e., 10.32 g $Ca(OH)_2$, 9.64 g 85 wt% H_3PO_4, 3.0 g SF, 3.0 g chitosan. SF powders of 3 g were added into a suspension containing 10.32 g $Ca(OH)_2$ and 120 g distilled water. A chitosan aqueous solution was prepared by dissolving 3 g chitosan powder into 117 g 2.0 wt% acetic solution, and subsequently mixed with 9.64 g 85 wt% H_3PO_4. The chitosan/H_3PO_4 solution was added dropwise into the SF/$Ca(OH)_2$ suspension. The pH of the mixture was 6.2 measured by a pH meter (PHS-3CT, Shanghai Dapu Instrument Co., Ltd., China), and then adjusted to be 9.0 by adding ammonium hydroxide in drops into the mixture. The reaction temperature was kept at 25 °C and the mixture was stirred at 800 rpm for 3 h, followed by three cycles of alternate centrifugation and water-washing to harvest the precipitates. The precipitates were vacuum-dried at 50 °C for 48 h and subsequently ground into fine powders using an agate mortar. Meanwhile, pure HA without SF and chitosan was prepared as a control sample by the same procedure. For mechanical tests, 1 g powder sample was compressed into a cylindrical tablet with a diameter of 12.5 mm and a height of 4.2–4.6 mm under a load of 10 MPa for 2 min.

2.2. Characterization of the materials

Crystalline phase composition of the as-prepared powders was confirmed by X-ray diffractometer (XRD) (RINT PC1, Rigaku Co.) with CuKα radiation. Fourier transform infrared (FT-IR) spectra were recorded using a spectrometer (Nicolet, AVATR360). A transmission electron microscope (TEM) (JEOL JEM-2100) was used to observe morphology of HA crystals. Thermogravimetric analysis (TGA) was performed in air between 25 and 1000 °C at a heating rate of 10 °C/min (TGA/SDTA851e, Mettler-Toledo, Inc.). The compressive strengths of tablet samples

were measured by a universal testing machine (AG-2000A, Shimadzu Co.) at a cross head speed of 2 mm/min. Five tablets were tested for each sample.

3. Result and discussion

As shown in Fig. 1, HA/CTS–SF composite and pure HA have similar XRD patterns. All the diffraction peaks are well defined and assigned to monophase crystalline HA only, since no peaks from other calcium phosphate phases are detected. It indicates that the involvement of chitosan and SF does not change crystallographic structure of HA in the composite. The two samples present notable line broadening and overlap of peaks, implying that the precipitated HA crystals have small size and low crystallinity similar to natural bone mineral (Murugan & Ramakrishna, 2004; Rhee & Tanaka, 2002). The poor crystalline nature of the prepared HA is possibly attributed to the low temperature procedure where the two samples were not subjected to sintering. The peaks in HA/CTS–SF composite are slightly broader as compared to pure HA, which is a sign for the decreased crystallinity of HA by the presence of the complex matrix.

FT-IR spectra of chitosan, SF, pure HA and HA/CTS–SF composite are shown in Figs. 2 and 3. Pure HA and the composite display a quite similar appearance with respect to the typical peaks of HA. The bands at 1092, 1033, 961, 603 and 565 cm^{-1} correspond to different modes of PO_4 group in HA (Rhee & Tanaka, 2002; Yamaguchi et al., 2001). The bands at 1452, 1423 and 874 cm^{-1} are derived from carbonate ions, suggesting that the precipitated HA contains carbonate ions (Gibson & Bonfield, 2002). No carbonate source was introduced into the starting materials, and the two samples were prepared in an atmospheric environment. It is reasonable to infer that the carbonate ions incorporated into HA stem from carbon dioxide gas in air. The band at 1638 cm^{-1} representing OH group of HA appears as a sharper peak in HA/CTS–SF, possibly ascribed to the overlap of OH group of HA and amide I band of SF. The characteristic β-sheet structure of SF is probed at 1634 cm^{-1} (amide I), 1519 cm^{-1} (amide II) and 1232 cm^{-1} (amide III) in Fig. 3a (Freddi et al., 1997). These amide bands are also observed in the composite (Fig. 3c) without notable peak shifts. In Fig. 3b, the bands at 1656, 1603, 1425, 1381 cm^{-1} are assigned to amide I (C═O), amino ($–NH_2$), CH deformation and CH_3 symmetric deformation in chitosan, respec-

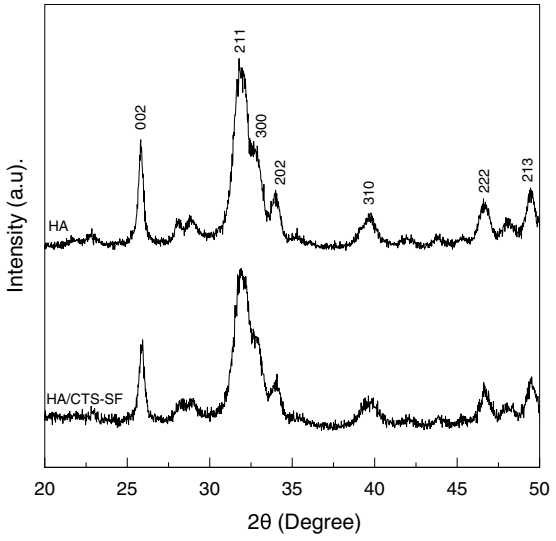

Fig. 1. XRD patterns of pure HA and HA/CTS–SF composite.

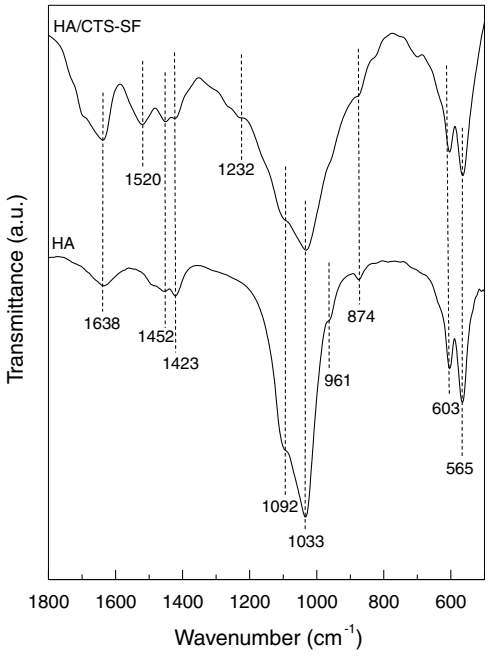

Fig. 2. FT-IR spectra of pure HA and HA/CTS–SF composite in the frequency range of 500–1800 cm^{-1}.

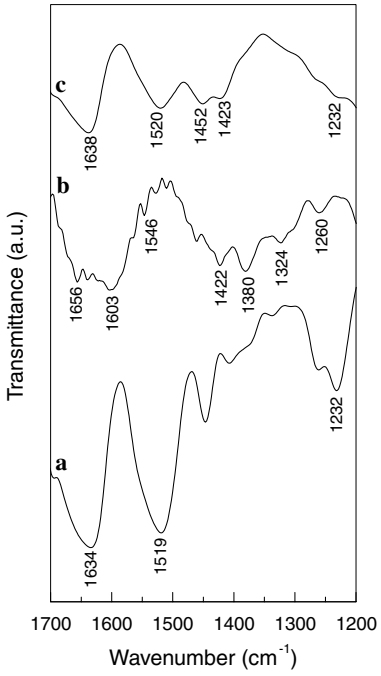

Fig. 3. FT-IR spectra of (a) silk fibroin, (b) chitosan, (c) HA/CTS–SF composite in the frequency range of 1200–1700 cm^{-1}.

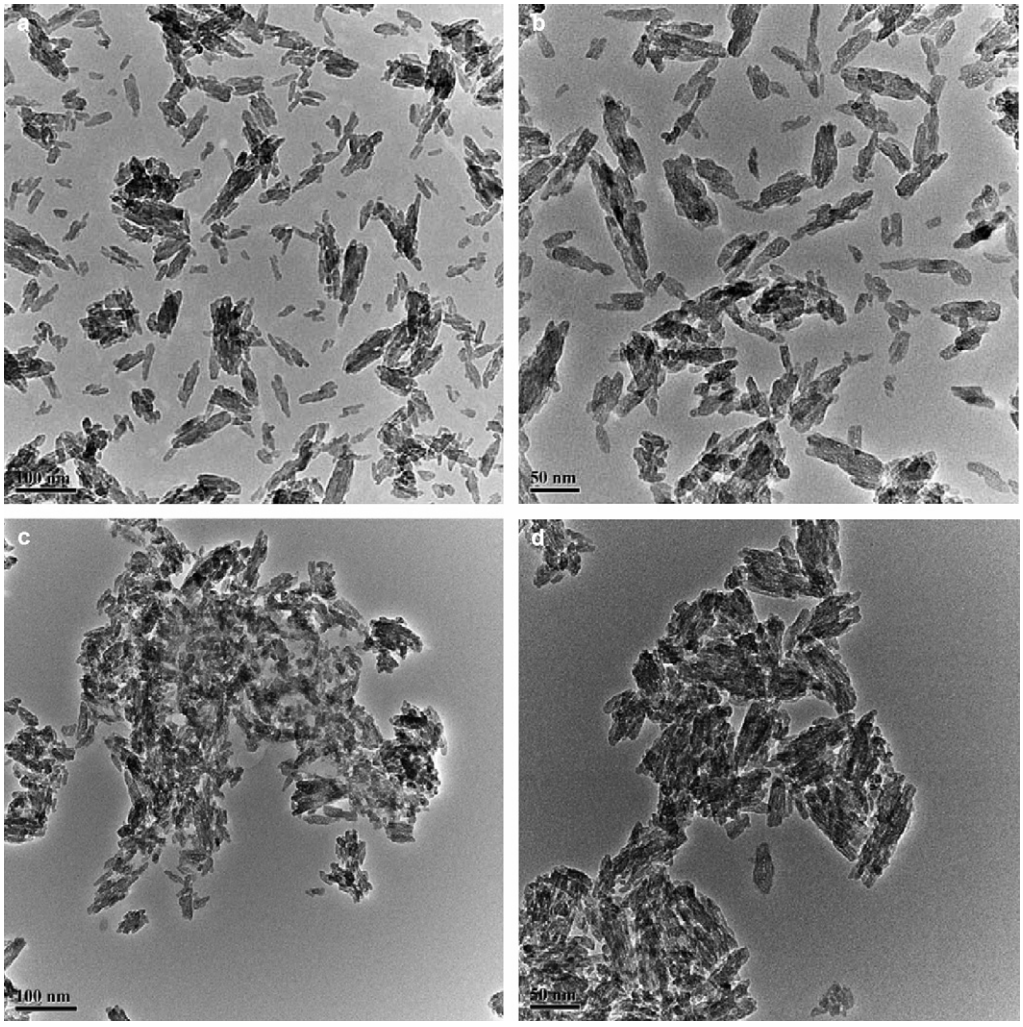

Fig. 4. TEM images of pure HA (a and b) and HA/CTS–SF composite (c and d).

tively (Qu, Wirsen, & Albertsson, 1999; Yamaguchi et al., 2001). These adsorption peaks are not easily detected or appear as weak shoulders in the composite. One possible reason is that SF presents very strong adsorption peaks particularly around 1400–1700 cm^{-1} compared to chitosan. As stated in some reports, there exist chemical interactions between the inorganic and organic components in HA-based composites, most likely occurring between Ca^{2+} and those negative charged functional groups in organic matrix such as COO^{-}, $-NH_2$, amide I and amide II (Kikuchi et al., 2001, 2004; Rhee & Tanaka, 2002; Yamaguchi et al., 2001). As to this study, we suggest that the chemical bonding may be formed between Ca^{2+} and the amino group of chitosan or the amide bands (amide I and amide II) of SF.

TEM images of the two samples are shown in Fig. 4. In pure HA and the composite, the elongated HA crystallites are envisioned as needle-like in shape with a typical size of 20–50 nm in length and about 10 nm in width. It implies that the morphology of HA crystallites is not altered by the complex organic matrix. The image of the crystallites in the composite is not as clear as that in pure HA. The obscure shadows are observed somewhere in the composite, attributed to the amorphous phases. This indicates the crystallinity of HA decreases with the addition of chitosan and SF, being in agreement with the above XRD result. The crystallites are in relatively well-dispersed state in pure HA in comparison with the severe agglomeration in the composite. HA nanocrystals spontaneously aggregate into bundles in both the cases. An apparent tendency is noticed in the composite that the aggregation is preferentially along *c* axis. This phenomenon is thought to be likely associated with the preferential self-assembly of HA crystallites along *c* axis, which has been revealed in several other studies (Rhee & Tanaka, 2002; Yamaguchi et al., 2001; Zhang et al., 2005). These findings demonstrate that the introduction of SF and chitosan intensifies the aggregation of HA crystals and promotes the aggregation along *c* axis.

The TG curves of the two samples, chitosan and SF are displayed in Fig. 5. The trace of pure HA (Fig. 5a) shows a continuous weight loss of 8% from 50 °C onward until 700 °C, and a notable weight loss in the range of 50–150 °C. The losses below 100 °C and around 120 °C can be ascribed to the evaporation of water (Sivakumar et al., 2002; Yamaguchi et al., 2001). There is no weight loss occurred above

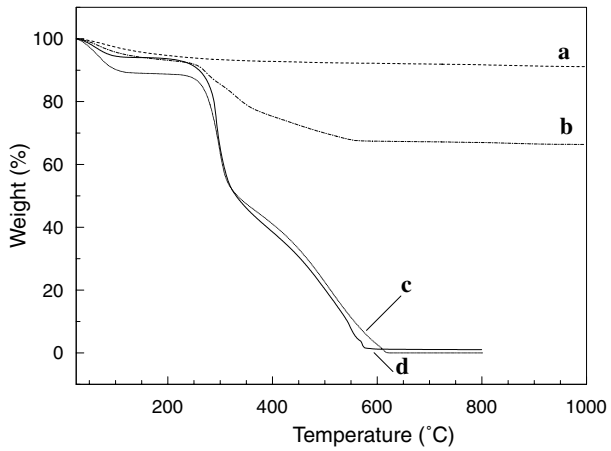

Fig. 5. TG thermograms of (a) pure HA, (b) HA/CTS–SF composite, (c) chitosan and (d) silk fibroin.

Table 1
Compressive strengths of pure HA and HA/CTS–SF composite (mean ± SD; $n = 5$)

Sample	Compressive strength (MPa)
HA	89.6 ± 2.8
HA/CTS–SF	179.3 ± 4.6

800 °C, suggesting that the precipitated HA is thermally stable at high temperature. It can be seen from the trace of HA/CTS–SF (Fig. 5b) that the sample weight decreases rapidly with temperature increasing, especially in the ranges of 50–120 °C assigned to the loss of water molecules, and 240–550 °C assigned to the thermal decomposition of organic macromolecules. There is no change found in the weight of the composite above 620 °C, indicating that the organic contents are decomposed completely at 620 °C. As confirmed from Fig. 5c and d, chitosan and SF are thermal stable up to 620 and 570 °C, respectively. The total weight loss for HA/CTS–SF composite is 32%, higher than that for pure HA (8%) due to the presence of chitosan and SF. The organic/inorganic weight ratio except water content for the composite is determined to be 28.9/71.1, almost consistent with the theoretical yield weight ratio of (chitosan and SF)/HA. The thermal analysis illustrates that chitosan and SF molecules have been well incorporated into the composite.

The compressive strengths of the two samples are given in Table 1. With the involvement of chitosan and SF, the compressive strength shows a notable increase, i.e., from 89.6 MPa for pure HA to 179.3 MPa for HA/CTS–SF. It is widely accepted that compressive strength for inorganic–organic hybrid materials can be viewed as an indication of the interfacial bonding strength between the mineral and organic components (Evans, Behiri, Currey, & Bonfield, 1990). In addition, the proper stress transfer occurring between the mineral phase and the organic matrix has a major effect on the mechanical properties of the composite materials (Sailaja et al., 2003). Regarding the present context, the chemical interaction and the intimate adhesion between HA and the complex organic matrix may account for the enhanced compressive strength.

4. Conclusions

HA/CTS–SF composite was obtained via a simple coprecipitation method at room temperature with chitosan and SF serving as a complex organic matrix. The inorganic component in the composite is identified as monophase poorly crystalline HA containing carbonate ions. The primary HA crystallites are needle-like and of 20–50 nm long and around 10 nm wide. FT-IR spectroscopy and TG thermal analysis confirm that chitosan and SF have been incorporated into the composite. The chemical interactions between the inorganic and organic constituents in the composite, probably take place via the chemical bonding between Ca^{2+} and the amino group of chitosan or the amide bands of SF. The involvement of chitosan and SF endows the composite with a higher compressive strength as compared to pure HA. These findings suggest that HA/CTS–SF composite may be a promising biomaterial for bone ingrowth and implant fixation.

Acknowledgments

This work was sponsored by the national natural science foundation of China (20236020, 20176009), the pre-973 project of China (2002CCA2200), the Scientific Research Foundation of State Education Ministry for the Returned Overseas Chinese Scholars (2005383), China Postdoctoral Science Foundation, the major basic research project of Shanghai (04DZ14002), the special project for key laboratory of Shanghai (04DZ05622) and the special project for nanotechnology of Shanghai. The authors gratefully acknowledge Wuxi Smiss Technol. Co., Ltd., China for its kind donation of silk fibroin powders.

References

Bigi, A., Panzavolta, S., & Roveri, N. (1998). Hydroxyapatite–gelatin films: a structural and mechanical characterization. *Biomaterials, 19*, 739–744.

Chang, M. C., Ikoma, T., Kikuchi, M., & Tanaka, J. (2002). The cross-linkage effect of hydroxyapatite/collagen nanocomposites on a self-organization phenomenon. *Journal of Materials Science: Materials in Medicine, 13*, 993–997.

Chang, M. C., Ko, C. C., & Douglas, W. H. (2003). Preparation of hydroxyapatite–gelatin nanocomposite. *Biomaterials, 24*, 2853–2862.

Du, C., Cui, F. Z., Zhang, W., Feng, Q. L., Zhu, X. D., & De Groot, K. (2000). Formation of calcium phosphate/collagen composites through mineralization of collagen matrix. *Journal of Biomedical Materials Research, 50*, 518–527.

Evans, G. P., Behiri, J. C., Currey, J. D., & Bonfield, W. (1990). Microhardness and Young's modulus in cortical bone exhibiting a wide range of mineral volume fractions, and in a bone analogue. *Journal of Materials Science: Materials in Medicine, 1*, 38–43.

Freddi, G., Monti, P., Nagura, M., Gotoh, Y., & Tsukada, M. (1997). Structure and molecular conformation of tussah silk fibroin films: effect of heat treatment. *Journal of Polymer Science Part B: Polymer Physics, 35*, 841–847.

Furuzono, T., Taguchi, T., Kishida, A., Akashi, M., & Tamada, Y. (2000). Preparation and characterization of apatite deposited on silk fabric using an alternate soaking process. *Journal of Biomedical Materials Research, 50*, 344–352.

Gibson, I. R., & Bonfield, W. (2002). Novel synthesis and characterization of an AB-type carbonate-substituted hydroxyapatite. *Journal of Biomedical Materials Research, 59*, 697–708.

Hench, L. L. (1991). Bioceramics: from concept to clinic. *Journal of the American Ceramic Society, 74*, 1487–1510.

Kikuchi, M., Itoh, S., Ichinose, S., Shinomiya, K., & Tanaka, J. (2001). Self-organization mechanism in a bone-like hydroxyapatite/collagen nanocomposite synthesized in vitro and its biological reaction in vivo. *Biomaterials, 22*, 1705–1711.

Kikuchi, M., Matsumoto, H. N., Yamada, T., Koyama, Y., Takakuda, K., & Tanaka, J. (2004). Glutaraldhyde cross-linked hydroxyapatite/collagen self-organization nanocomposites. *Biomaterials, 25*, 63–69.

Mann, S., & Ozin, G. A. (1996). Synthesis of inorganic materials with complex form. *Nature, 382*, 313–318.

Murugan, R., & Ramakrishna, S. (2004). Bioresorbable composite bone paste using polysaccharide based nano hydroxyapatite. *Biomaterials, 25*, 3829–3835.

Nunes, C. R., Simske, S. J., Sachdeva, R., & Wolford, L. M. (1997). Long-term ingrowth and apposition of porous hydroxylapatite implants. *Journal of Biomedical Materials Research, 36*, 560–563.

Park, S. J., Lee, K. Y., Ha, W. S., & Park, S. Y. (1999). Structural changes and their effect on mechanical properties of silk fibroin/chitosan blends. *Journal of Applied Polymer Science, 74*, 2571–2575.

Qu, X., Wirsen, A., & Albertsson, A. C. (1999). Structural change and swelling mechanism of pH-sensitive hydrogels based on chitosan and D,L-lactic acid. *Journal of Applied Polymer Science, 74*, 3186–3192.

Rhee, S. H., & Tanaka, J. (2002). Self-assembly phenomenon of hydroxyapatite nanocrystals on chondroitin sulfate. *Journal of Materials Science: Materials in Medicine, 13*, 597–600.

Rusu, V. M., Ng, C. H., Wilke, M., Tiersch, B., Fratzl, P., & Peter, M. G. (2005). Size-controlled hydroxyapatite nanoparticles as self-organized organic–inorganic composite materials. *Biomaterials, 26*, 5414–5426.

Sailaja, G. S., Velayudhan, S., Sunny, M. C., Sreenivasan, K., Varma, H. K., & Ramesh, P. (2003). Hydroxyapatite filled chitosan-polyacrylic acid polyelectrolyte complexes. *Journal of Materials Science, 38*, 3653–3662.

Sivakumar, M., Manjubala, I., & Rao, P. K. (2002). Preparation, characterization and in-vitro release of gentamicin from coralline hydroxyapatite–chitosan composite microspheres. *Carbohydrate Polymers, 49*, 282–288.

Song, J., Saiz, E., & Bertozzi, C. R. (2003). A new approach to mineralization of biocomposite hydrogel scaffolds: an efficient process toward 3-dimensional bonelike composites. *Journal of the American Chemical Society, 125*, 1236–1243.

Stupp, S. I., & Braun, P. V. (1997). Molecular manipulation of microstructures: biomaterials, ceramics, and semiconductors. *Science, 277*, 1242–1248.

Wang, L., Nemoto, R., & Senna, M. (2002). Microstructure and chemical states of hydroxyapatite/silk fibroin nanocomposites synthesized via a wet-mechanochemical route. *Journal of Nanoparticle Research, 4*, 535–540.

Wang, L., Nemoto, R., & Senna, M. (2004). Changes in microstructure and physico-chemical properties of hydroxyapatite–silk fibroin nanocomposite with varying silk fibroin content. *Journal of the European Ceramic Society, 24*, 2707–2715.

Yamaguchi, I., Tokuchi, K., Fukuzaki, H., Koyama, Y., Takakuda, K., Monma, H., et al. (2001). Preparation and microstructure analysis of chitosan/hydroxyapatite nanocomposites. *Journal of Biomedical Materials Research, 55*, 20–27.

Zhang, W., Liao, S. S., & Cui, F. Z. (2003). Hierarchical self-assembly of nanofibrils in mineralized collagen. *Chemistry of Materials, 15*, 3221–3226.

Zhang, L., Li, Y. B., Yang, A. P., Peng, X. L., Wang, X. J., & Zhang, X. (2005). Preparation and in vitro investigation of chitosan/nano-hydroxyapatpite composite used as bone substitute materials. *Journal of Materials Science: Materials in Medicine, 16*, 213–219.